J|A|C|S ARTICLES

Published on Web 11/13/2009

Tuning of Refractive Indices and Optical Band Gaps in Oxidized Silicon Quantum Dot Solids

Jin-Kyu Choi,[†] Seunghyun Jang,[‡] Honglae Sohn,*[,‡] and Hyun-Dam Jeong*[,†]

Department of Chemistry, Chonnam National University, Gwangju-si 500-757, Korea, and Department of Chemistry, Chosun University, Gwangju-si 501-759, Korea

Received August 11, 2009; E-mail: hdjeong@chonnam.ac.kr; hsohn@chosun.ac.kr

Abstract: This laboratory has initiated compelling research into silicon quantum dot (Si QD) solids in order to utilize their synergetic benefits with quantum dot solids through fabrication of Si QD thin films. The issues of oxidation concerning the Si QD thin films were confirmed using Fourier transform infrared spectroscopy (FT-IR) and X-ray photoelectron spectroscopy (XPS). The refractive index value of the Si QD thin film at a 30 °C curing temperature was 1.61 and 1.45 at 800 °C due to complete oxidation of the Si phases. The optical band gap values of 5.49−5.90 eV corresponded to Si phases with diameters between 0.82 and 0.74 nm, dispersed throughout the oxidized Si QD thin films and modeled by Si molecular clusters of approximately 14 silicon atoms. The photoluminescence (PL) energy (2.64−2.61 eV) in the proposed Si QD thin films likely originated from the Si═O bond terminating the Si molecular clusters.

Introduction

While bulk Si has very weak luminescence due to its indirect band gap, nanosized silicon quantum dots (Si QDs) possess more efficient luminescence. When carriers are confined in the real space of nanosized Si QDs, the band structure of the Si QDs become more direct given their wave functions being spread out into reciprocal space.[1,2] Silicon QDs are also nontoxic and cheap when compared to well-investigated II−VI semiconductors that contain cadmium. In addition, Si QDs are expected to integrate easily into well-established industrial silicon processes. Nevertheless, in recent years, the exact type of collective properties that arise when semiconductor quantum dots (QDs) are assembled into two- or three-dimensional arrays has drawn much interest.[3] The term “quantum dot solids” is used to indicate three-dimensional assemblies of semiconductor QDs. The opto-electronic properties of the quantum dot solids are known to depend on the electronic structure of the individual quantum dot building blocks and on their electronic interactions. Due to quantum confinement effects, semiconductor QDs are characterized by discrete energy levels, including S, P, and D levels. A detailed theoretical framework for the transport characteristics of QD solids has been presented in a strong coupling regime, indicating higher tunneling rates and electronic interactions from dot to dot.[4] Practically, this laboratory realized the importance of the electronic interactions within QD solids from its recent investigation of spin-coated CdS thin film transistors (TFTs) where the high mobility (48 $cm^2\ V^{-1}\ s^{-1}$) of the CdS QD films could be understood by assuming a significant overlap of electronic wave functions.[5] Quantum dot solids with controlled and variable electron densities are predicted to be quite useful in the field of opto-electronic switches, LEDs, lasers, and solar cells.

Recently, in order to utilize the synergetic benefits of Si QDs and quantum dot solids, this laboratory investigated the optical properties of “Si QD solids”. There still exist, however, numerous ambiguities regarding this topic, including surface oxidation of Si QD surfaces, electronic communication between QDs, and the extent to which the photoluminescence properties are affected by the synthetic and treatment conditions. Recently, H. Sohn et al. performed interesting work on the synthesis of Si QDs,[6] where *n*-butyl-capped Si QDs possessed an average diameter of approximately 6.5 nm. These Si QDs were very soluble in organic solvents such as tetrahydrofuran (THF), a major prerequisite for generating Si QD solid thin films using the conventional spin-coating process.

However, unexpectedly, attempts to reproduce H. Son’s synthesis in this laboratory failed because of two problems. The first involved oxidation of the Si QD precursor either during its synthesis or under storage in diethyl ether prior to use for spin-coating, as depicted in Figure 1a. This oxidation was clearly confirmed by FT-IR (Figure 2a). The second problem arose during the filmmaking process (consisting of the spin-coating and curing processes), during which the Si QD thin films were easily prone to further oxidation under low vacuum conditions (pressure $\leq 1.0 \times 10^{-2}$ Torr), as summarized in Figure 1b. This occurred regardless of whether the capped *n*-butyl groups existed or decomposed out over the wide range of curing temperatures. These findings contradict the authors’ original contention of the Si QD surface *n*-butyl groups, completely precluding oxidation at low temperatures (<400 °C); as such, oxidation is possible

[†] Chonnam National University.
[‡] Chosun University.

(1) Brus, L. *J. Phys. Chem.* **1994**, *98*, 3575.
(2) Hybersten, M. S. *Phys. Rev. Lett.* **1994**, *72*, 1514.
(3) Vanmaekelbergh, D.; Liljeroth, P. *Chem. Soc. Rev.* **2005**, *34*, 299.
(4) Remacle, F. *J. Phys. Chem. A* **2000**, *104*, 4739.
(5) Seon, J. B.; Lee, S.; Kim, J.; Jeong, H. D. *Chem. Mater.* **2009**, *21*, 604.
(6) Jang, S.; Kim, J.; Koh, Y.; Jung, K.; Woo, H.-G.; Sohn, H. *J. Nanosci. Nanotechnol.* **2009**, in press.

10.1021/ja9065656 CCC: $40.75
© 2009 American Chemical Society

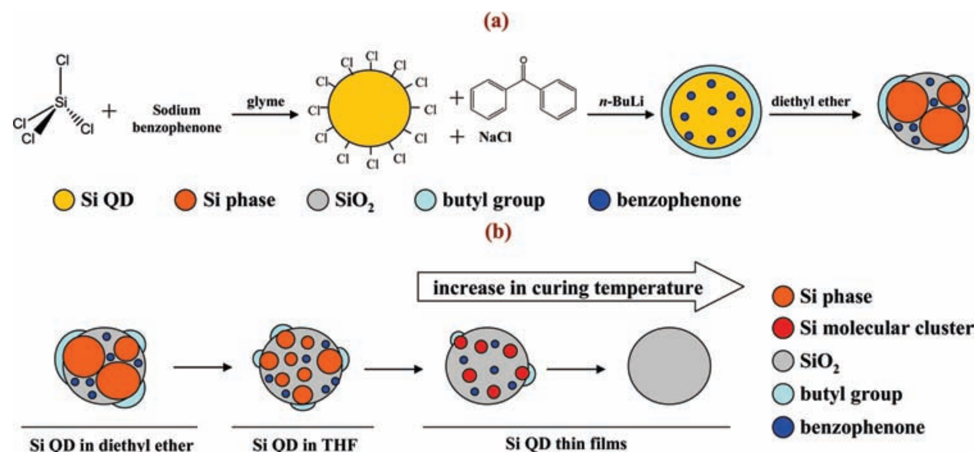

Figure 1. (a) Reaction scheme of the Si QD. The Si QD precursor was oxidized either in its synthetic process or when stored in diethyl ether prior to use for the spin-coating process. (b) The Si QD thin films were easily further oxidized during the spin-coating and curing processes.

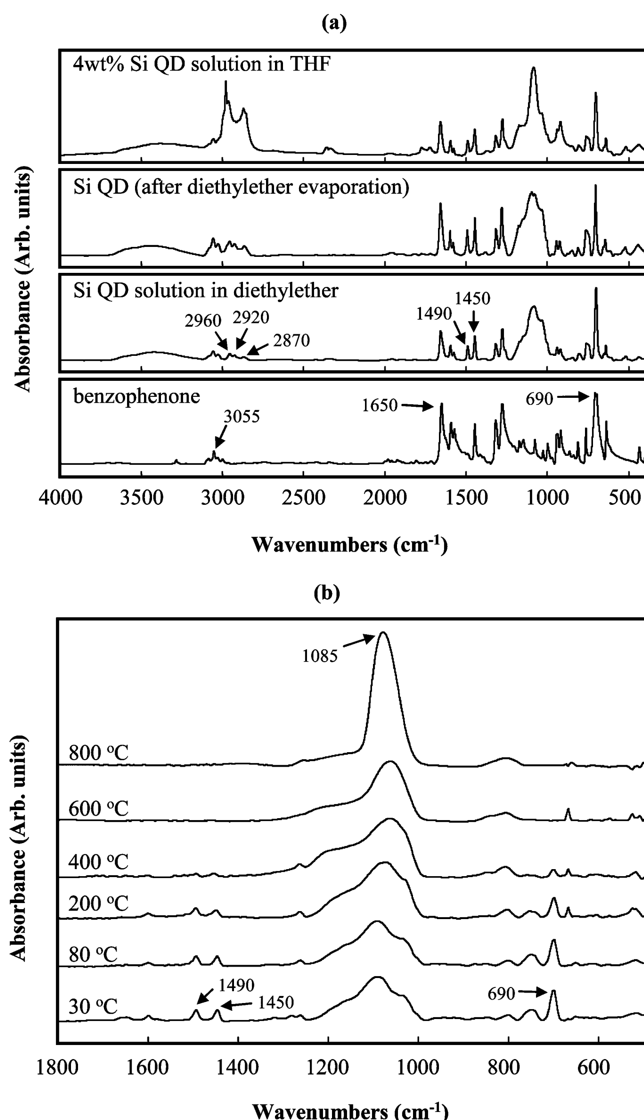

Figure 2. FT-IR results. (a) The Si QDs in the solutions had been oxidized prior to spin-coating of the Si QD thin films. (b) Over 400 °C, organic groups, including benzophenone and *n*-butyl, were removed from the Si QD thin films, forming SiO_2 phases.

only after film curing at higher temperatures (≥400 °C), when decomposition or degassing out of the *n*-butyl groups was observed. As a result, the oxidized Si QD thin films were synthesized from the oxidized Si QD precursors, not from the pure Si QDs as originally predicted. Consequently, we have hardly performed deep investigation on the electronic communications, control of luminescence properties due to the control of surface oxidation, and the effect of the capped-alkyl groups of the Si QD solids, which had been originally planned.

Even though the original research goals could not be attained, interesting optical properties were measured in the oxidized Si QD thin films with potential application in future photonic applications and fundamental studies on dielectrics. In this article, it is proposed that these optical properties are due to subnanometer silicon phases dispersed in the oxidized Si QDs, branded "silicon molecular clusters" by the authors to distinguish them from Si QDs.

Experimental Section

Synthesis of *n*-Butyl-Terminated Si QDs. Silicon quantum dots (Si QDs) terminated with the *n*-butyl group were synthesized following the procedure described by Jang et al.[6] Sodium metal (99%), benzophenone (99%), silicon tetrachloride ($SiCl_4$, 99.999%), and *n*-butyllithium (1.6 M in hexane) were supplied by Sigma-Aldrich and used without further purification. Ethylene glycol dimethyl ether (glyme) was dried and distilled from a sodium−potassium (Na−K) alloy under argon gas. Sodium metal (523.9 mg, 22.8 mmol) and benzophenone (4.154 g, 22.8 mmol) were added to a Schlenk flask in a drybox under argon. Freshly distilled and degassed glyme (60 mL) was added to the solids, and the mixture was stirred overnight. The mixture was added to silicon tetrachloride (2.23 g, 13.0 mmol) in 100 mL of glyme and stirred for 2 h at room temperature. The bright yellow solution at the top of the flask was transferred to a new Schlenk flask and vacuum-dried to remove the benzophenone. Then, 100 mL of distilled glyme and 8.2 mL of *n*-butyllithium were added to the flask and stirred overnight. The product was extracted with hexane and the extract rinsed with water. Finally, *n*-butyl-terminated Si QDs were obtained, after the removal of hexane and any residual benzophenone, and stored in diethyl ether until use.

Preparation of a 4 wt % Si QD Solution in Tetrahydrofuran. Silicon quantum dots predissolved in diethyl ether were evaporated under vacuum at room temperature for 10 min to obtain the Si QDs. Tetrahydrofuran (THF, 2.4 g) was then added to the Si QDs (0.1 g). After stirring for 5 min, a 4 wt % Si QD solution was obtained.

Preparation of Si QD Thin Films. The 4 wt % Si QD solution in THF was filtrated (PTFE, 0.25 μm) and spin-coated on p-type Si(100) wafers (resistivity: 1−30 Ω·cm, thickness: 525 nm) at 2000

rpm. The Si wafers were purchased from Silicon Valley Microelectronics, Inc. Under a vacuum of approximately 1.0×10^{-2} Torr for 30 min, the thin films on the Si wafers were cured at the following temperatures: (1) 30 °C; (2) 80 °C; (3) 200 °C; (4) 400 °C; (5) 600 °C; (6) 800 °C.

Characterization. Fourier transform infrared spectroscopy (FT-IR) was implemented to investigate the molecular structure of the Si QD precursor solutions and the Si QD thin films as a function of curing temperature. The measurements were conducted on a Nicolet 380 spectrometer operated in the mid-IR range of 4000−400 cm^{-1}, with all spectra obtained at a spectral resolution of 16 cm^{-1} in the transmittance mode. To investigate compositional changes with increasing curing temperature, X-ray photoelectron spectroscopy (XPS) measurements were conducted on a MultiLab 2000 using a Mg Kα (1253.6 eV) source at a pass energy of 20 eV under a pressure of 1.0×10^{-9} Torr. An Ar^+ ion gun sputtering of 2 min at a power of 2 kV and 1.3 μA was used for a brief cleaning of the surface of the samples prior to XPS measurements. The optical properties of the Si QD solution (THF) and the Si QD thin films were investigated. The thickness and refractive indices of the Si QD thin films were measured by spectroscopic ellipsometry (SE) with an M2000D (J. A. Wollam Co. Inc., U.S.A.). Ultraviolet visible (UV−vis) absorption spectroscopy was performed in a range of 200−1000 nm with a SCINCO S-3150. Photoluminescence spectroscopy was performed using a He−Cd (Kimmon Electric Co., IK3501R-G, Japan) light source at 325 nm with 50 mW power and an intensified photodiode array detector (IRY1024, Princeton Instrument Co., U.S.A.) to investigate the fluorescence properties of the Si QD precursors and thin films. Transmission electron microscopy (FETEM, FEI, Tecnai F30 Super-Twin, Netherlands) analysis was performed to investigate the microstructure of the thin films. Cross-sectional TEM specimens were prepared through mechanical polishing followed by Ar ion milling (GATAN, PIPS 691) for electron transparency. Film crystallinity was measured with an X-ray diffractometer (RIGAKU, D/MAX-2500, Japan) equipped with a Cu Kα source at 40 kV and 300 mA.

Results and Discussion

Benzophenone showed specific infrared absorption peaks (Figure 2a): the peak at 3055 cm^{-1} is attributed to the stretching of the sp^2-hybridized C−H; the peak at 1650 cm^{-1} is attributed to the stretching of the conjugated C═O; the peaks at 1600−1400 cm^{-1} are attributed to the stretching of C═C in the aromatic groups; the peak at 690 cm^{-1} is attributed to the bending of C−H in the monosubstituted aromatic groups.[7] From the peak comparisons in Figure 2a, it was evident that the benzophenone used during the synthetic process remained in the Si QD and its subsequent solutions (diethyl ether or THF). The peaks of the *n*-butyl capping groups on the Si QD surfaces were observed at 2960, 2920, 2870, 1490, and 1450 cm^{-1}, all attributed to $C-CH_2$ and terminal $-CH_3$ vibrations.[6,8] The peaks at 1100−1000 cm^{-1} were attributed to the Si−O stretching detected in the Si QDs and its solution (diethyl ether or THF),[8] indicating that they had already been oxidized to form SiO_2 prior to spin-coating of the Si QD thin films. The FT-IR spectra of the Si QD thin films cured under low-vacuum conditions at various temperatures are shown in Figure 2b. The Si QD thin films cured below 400 °C showed peaks from benzophenone and *n*-butyl groups as mentioned above, indicating their existence in the Si QD thin films. However, over 400 °C, the organic groups (benzophenone and *n*-butyl) were removed from the Si QD thin films. As the temperature increased, the peak intensity at 1085 cm^{-1} attributed to Si−O stretching increased, indicating formation of SiO_2 *via* oxidation.

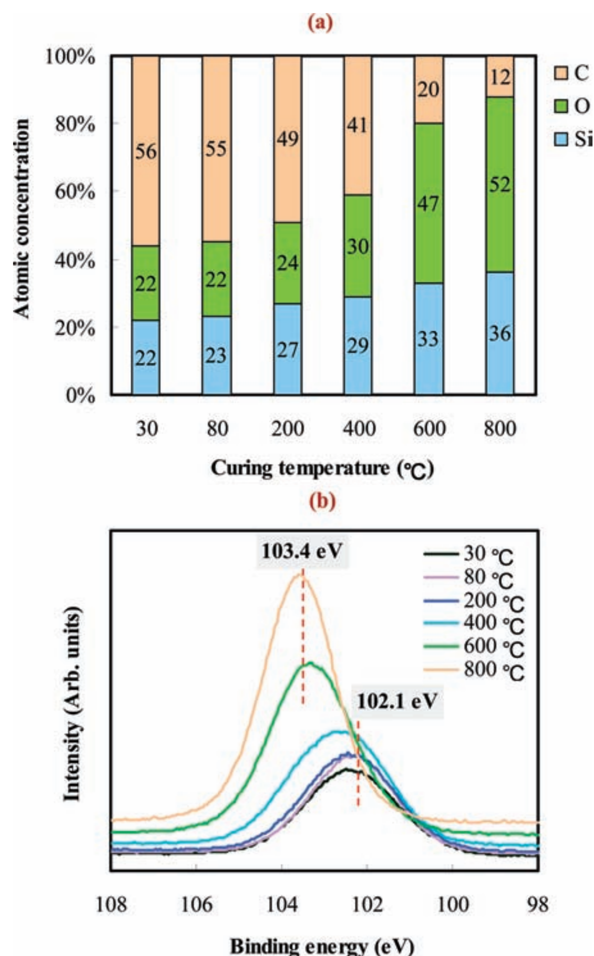

Figure 3. (a) XPS quantification results. As the curing temperature increased, the atomic concentration of oxygen increased, and simultaneously, that of the carbon representing the organic capping groups of the Si QD surfaces decreased, indicating oxidation of Si QD thin films. (b) Si 2p high-resolution spectra. As the curing temperature increased, the Si 2p binding energy increased from 102.1 eV for the Si QD thin film cured at 30 °C to 103.4 eV for the Si QD thin film cured at 800 °C. The peak at 102.1 eV can be assigned to $Si(-Si-)_2(-O-)_2$.

Figure 3 shows the variation in the films' chemical composition according to changes in the temperature applied to the Si QD thin films. In Figure 3a, the overall trend is that higher temperatures promote oxidation of the Si QD thin films. As the curing temperature increased, the atomic concentration of oxygen increased, while simultaneously that of the carbon from the organic capping groups on the Si QD surface decreased, signifying oxidation of the Si QD thin films. In particular, comparing the results of 30−400 °C with those at 600−800 °C, the decrease in the carbon concentration and the increase in oxygen concentration occurred rapidly because organic groups, including the *n*-butyl, are almost wholly degraded at temperatures above 400 °C. Thus, the absence of *n*-butyl groups capping the surface of the Si QD is thought to accelerate oxidation of the Si QD. The Si 2p peaks that were charge-calibrated by positioning the C 1s peak to 284.6 eV of the Si QD thin films are shown in Figure 3b. As the curing temperature increased, the Si 2p binding energy increased from 102.1 eV for the Si QD thin film cured at 30 °C to 103.4 eV for the Si QD thin film cured at 800 °C. The peaks at 102.1 and 103.4 eV indicated the $Si(-R)_2(-O-)_2$ and $Si(-O-)_4$ (SiO_2), whose

(7) Pavia, D. L.; Lampman, G. M.; Kriz, G. S.; Vyvyan, J. R. *Introduction to Spectroscopy* , 4th ed.; Brooks/Cole: Belmont, CA, 1996; p 56.
(8) Yang, C. S.; Bley, R. A.; Kauzlarich, S. M.; Lee, H. W. H.; Delgado, G. R. *J. Am. Chem. Soc.* **1999**, *121*, 5191.

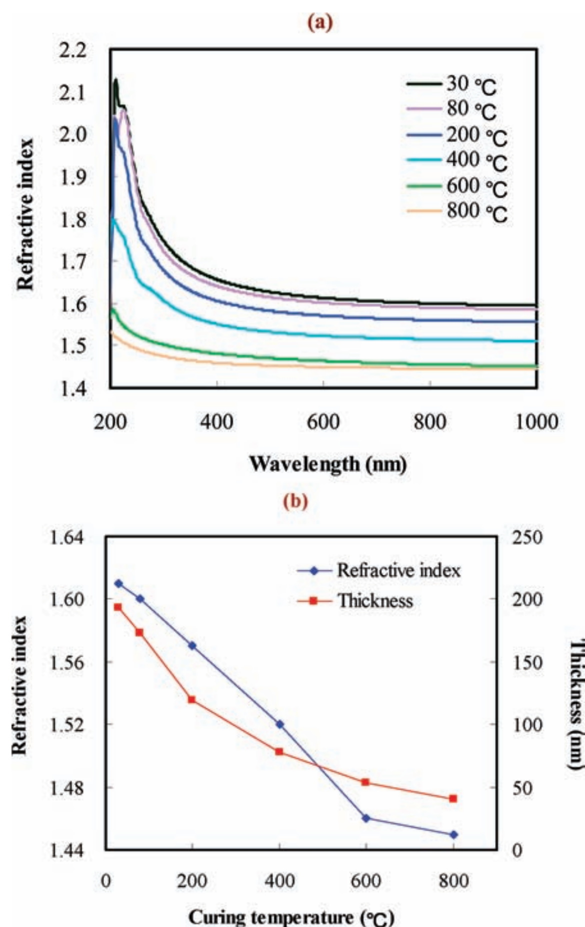

Figure 4. SE results. (a) The variation in the refractive indices and thicknesses of the Si QD thin films according to curing temperatures is shown. (b) As the oxidation proceeded with increasing curing temperature, the decrease in refractive index due to formation of the SiO_2 phases overwhelmed this increase due to film densification.

respective Si oxidation numbers were +2 and +4.[9] The Si oxidation number proportional to the binding energy increased with increasing curing temperature. Notwithstanding, the peak at 102.1 eV can also be assigned to $Si(-Si-)_2(-O-)_2$, since it has the same chemical environment in the sense of XPS as $Si(-R)_2(-O-)_2$, indicating the same electron density of the silicon atom. This kind of silicon atom could constitute the Si molecular cluster embedded in the oxidized Si QD thin films discussed below (Figure 6b). Presently, silicon atoms of 102.1 eV ensure the possibility of the existence of a silicon phase modeled upon the silicon molecular cluster in this article. The binding energy of the silicon phase was quite different from that (99 eV) of bulk silicon (Si_∞).[10] Thereupon, it is the deduction of the authors that the Si phases of the Si QD thin film cured at 30 °C gradually decrease with increasing curing temperature. Eventually, at a curing temperature of 800 °C, the Si phases of the Si QD thin film are completely removed and oxidized to form SiO_2.

The variation in the refractive index and thickness of the Si QD thin films according to the curing temperatures, is shown in Figure 4. The decrease in the thickness values indicated densification of the thin films, caused mainly by the decomposition and elimination of the *n*-butyl groups and benzophenone (Figure 2 and Figure 3). The organic groups had molecular free volumes, and the inorganic components (such as SiO_2 and silicon phases in the oxidized Si QDs) were densely close-packed. Accordingly, film shrinkage was expected to induce a necessarily higher film density. However, as shown in Figure 4, the refractive index values were found to decrease as the curing temperature increased (1.61 for 30 °C, while 1.45 for 800 °C), which was quite irregular as refractive index is typically proportional to film density. This inconsistency can be understood by considering the growth of the SiO_2 phases at the higher curing temperatures, which can be realized quantitatively through the following arguments. In the Bruggemann effective medium approximation, the effective dielectric function of a composite material of two components is obtained by solving the following equation:[11]

$$f_A\frac{\tilde{\varepsilon}_A-\tilde{\varepsilon}}{\tilde{\varepsilon}_A+2\tilde{\varepsilon}}+f_B\frac{\tilde{\varepsilon}_B-\tilde{\varepsilon}}{\tilde{\varepsilon}_B+2\tilde{\varepsilon}}=0$$

where f_A and f_B are the fractions of components A and B, $\tilde{\varepsilon}_A$ and $\tilde{\varepsilon}_B$ are the complex dielectric functions of components A and B, and $\tilde{\varepsilon}$ is the effective dielectric function of the composite material. If the composite material is assumed to consist of Si and SiO_2 phases, this equation is converted accordingly with refractive index values of 632.8 nm:

$$f_A\frac{n_{Si}^2-n^2}{n_{Si}^2+2n^2}+f_B\frac{n_{SiO_2}^2-n^2}{n_{SiO_2}^2+2n^2}=0$$

The refractive index of crystalline silicon and amorphous SiO_2 were respectively 3.882 and 1.457 at 632.8 nm.[12] The refractive index of the Si phase, whose existence was expected from the XPS results (Figure 3b), in the Si QD thin films herein, was surely lower than that of bulk crystalline silicon given its smaller size. This was possible by considering certain calculation results indicating that the static dielectric constant decreased with decreasing Si nanoparticle size.[13,14] Thus, it is the assumption of the authors that the refractive indices of the Si phases are located between 3.882 and 1.457. Then, as the curing temperature increased, the relative fraction of the SiO_2 phases increased, and that of the silicon phases decreased. Namely, as oxidation proceeds with increasing curing temperature, the decrease in refractive index due to the formation of the SiO_2 phases overwhelms its increase attributed to film densification.

Figure 5 shows UV−vis absorption results for the Si QD thin films for obtaining the optical band gap value. For direct band gap materials, the interband absorption was described by the following equation:[15]

$$\alpha h\nu = A(h\nu - E_g)^{1/2}$$

(9) Alexander, M. R.; Short, R. D.; Jones, F. R.; Michaeli, W.; Blomfield, C. J. *Appl. Surf. Sci.* **1999**, *137*, 179.
(10) Nordberg, R.; Brecht, H.; Albridge, R. G.; Fahlman, A.; Van Wazer, R. J. *Inorg. Chem.* **1970**, *9*, 2469.
(11) Tompkins, H. G.; McGahan, W. A. *Spectroscopic Ellipsometry and Reflectometry*; John Wiley & Sons: New York, 1999; p 126.
(12) Tompkins, H. G. *A User's Guide to Ellipsometry*; Academic Press: Boston, 1993; p 253.
(13) Wang, L. W.; Zunger, A. *Phys. Rev. Lett.* **1994**, *73*, 1039.
(14) Weissker, H.-Ch.; Furthmüller, J.; Bechstedt, F. *Phys. Rev. B* **2004**, *69*, 115310.
(15) Tauc, J.; Abrahám, A.; Zallen, R.; Slade, M. *J. Non-Cryst. Solids* **1970**, *4*, 279.

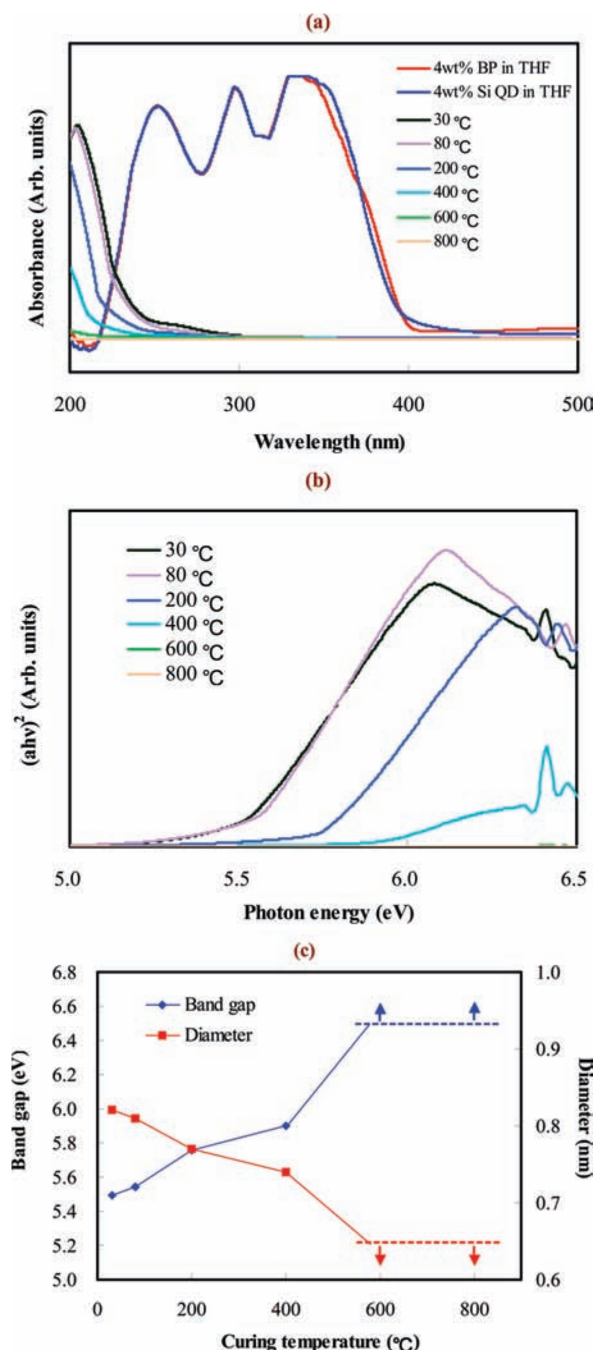

Figure 5. (a) UV−vis absorption spectra of the Si QD and Si QD thin films. (b) Tauc plot of the Si QD thin films obtained from their UV spectra. The Tauc plot of the Si QD thin films cured at 600 and 800 °C is not shown due to being beyond the detection limit (6.49 eV). (c) Energy gap of Si QD thin films.

where α is the optical absorption coefficient, $h\nu$ is photon energy, A is a constant, and E_g is the optical band gap energy. The band gap value of the Si QD thin film cured at 30 °C was estimated to be 5.49 eV using the Tauc plot (Figure 5b). The absorption spectrum of the Si QD precursor (4 wt % Si QD in THF) was hidden by chemisorbed benzophenone molecules. As such, no conclusion regarding the UV−vis absorption of the Si QD precursor could be made. The optical band gap originated from the difference in the energy of the lowest unoccupied state and the highest occupied state in the Si QDs, which is well-fitted by the following equation:[16]

$$E_g(d) = \varepsilon_c(d) - \varepsilon_v(d)$$

$$\varepsilon_c(d) = \varepsilon_c(\infty) + \frac{1}{a_c d^2 + b_c d + c_c}$$

$$\varepsilon_v(d) = \varepsilon_v(\infty) - \frac{1}{a_v d^2 + b_v d + c_v}$$

where $\varepsilon_c(\infty)$ and $\varepsilon_v(\infty)$ are the bulk band edges and a_c, b_c, c_c, a_v, b_v, and c_v are fitting parameters equaling 0.20321, 0.05673, 0.17815, 0.15001, 0.54779, and 0.07477, respectively. Using this equation, an optical band gap value of 5.49 eV corresponded to the Si phase of a diameter of 0.82 nm. The diameter was far less than that (6.5 nm) of the oxidized Si QD precursor. As a result of this, the authors tentatively assume that the Si phase is dispersed in the oxidized Si QD precursor (Figure 1). The Si phase is henceforth designated a "Si molecular cluster" since the diameter of 0.82 nm corresponded to roughly 14 silicon atoms based on simple cluster calculations (Figure 6a). The possibility of tetrahedrally bonded Si clusters has been proposed in the Si^+-implanted and annealed SiO_2 films, where various chemical species such as −O, −H, and −OH groups were attached to the unsatisfied chemical valences of the cluster and acted as luminescent entities from 2.7 to 3.0 eV.[17] As the curing temperature increased, the optical band gap value increased slightly within the range of 30−400 °C (Figure 5b). At a curing temperature of 400 °C, the diameter of the Si molecular cluster embedded in the oxidized Si QD was estimated to be 0.74 nm, where the optical band gap was 5.90 eV (a 7.5% increase from that for 30 °C). At higher curing temperatures, the optical band gap was not detected in the wavelength ranges of the present experiment (upper detection limit = 6.49 eV), possibly indicating the disappearance of the Si molecular clusters accompanying full oxidation.

Figure 7a shows the photoluminescence (PL) spectra for the Si QD thin films cured under low-vacuum conditions with those

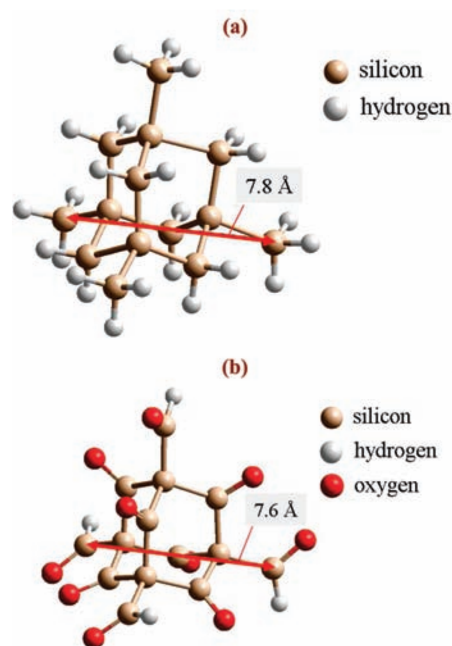

Figure 6. (a) Si molecular cluster modeling of the silicon phase of about 0.8 nm dispersed in oxidized Si QD thin films. The outer surface was a terminated Si−H bond. Geometry optimization was performed using a Polak−Ribiere algorithm in Hyperchem 8.0. (b) The Si−H termination was replaced with the Si=O bond and optimized again.

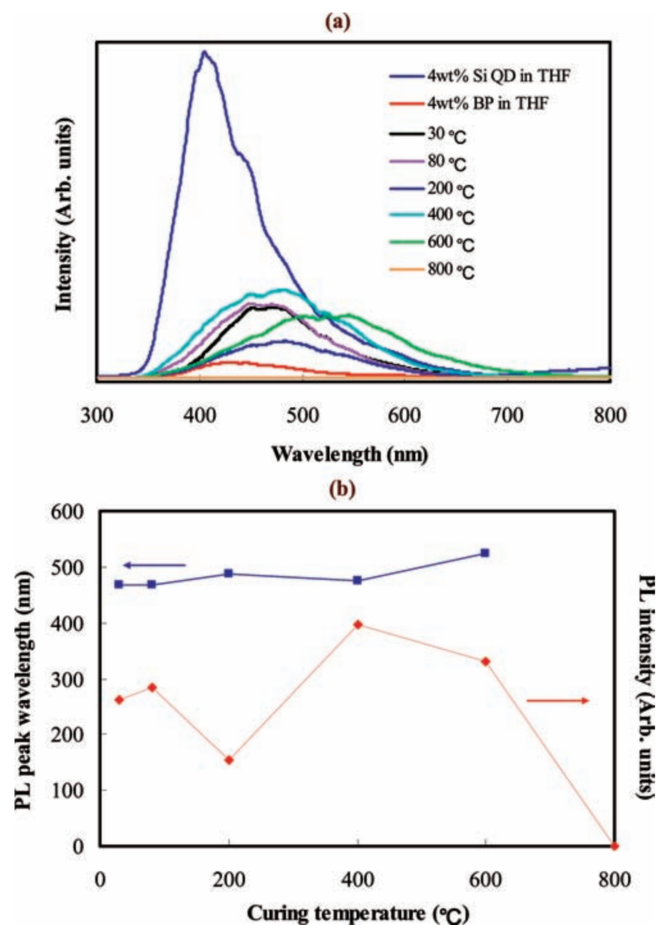

Figure 7. (a) PL spectra of the Si QD and Si QD thin films. (b) Variation of PL peak energies (PL peak wavelength) and intensities as a function of curing temperature.

of the 4 wt % benzophenone solution (THF) and 4 wt % Si QD solution (THF). The energies of the PL peaks of the Si QD thin films were red-shifted to 2.64−2.61 eV (470−475 nm) at 30−400 °C and 2.39 eV (520 nm) at 600 °C from 3.07 eV (405 nm) of the Si QD in THF, which has yet to be interpreted (Figure 7a and 7b). Within the range of 30−400 °C, the PL energy changed by just 1.1%, while the optical band gap changed by 7.5%, as mentioned above. Furthermore, at 600 °C, where the optical band gap was beyond the detection limit, indicating at least 6.49 eV (18% increase from that for 30 °C), the PL energy was measured at 2.39 eV (520 nm), 9% lower than that at 30 °C. The PL peak positions were not significantly changed as the curing temperature increased when compared with the optical band gap values. This is very unusual when recalling that both UV absorption and photoluminescence originated from the interband transition.

This strange phenomenon was similarly predicted in a study of electronic states and luminescence in porous silicon quantum dots,[18] where the PL energy was eventually saturated near 2.1 eV (590 nm) with increasing air exposure time. In this particular model, in the case that a Si cluster is passivated by hydrogen, recombination of electrons and holes for luminescence transpired *via* free exciton states for all sizes and the PL energy was equal to the free exciton band gap and followed the quantum confinement effect, which cannot explain the saturation of the PL energy near 2.1 eV. However, it was also reported that if the Si cluster is passivated by oxygen, a stabilized electronic state (or even trapped exciton) formed due to the Si=O covalent bond, explaining the saturation of the PL energy. When the silicon crystallites were very small (≤2.0 nm), the Si=O bond at the Si/SiO_2 interface was the origin of the photoluminescence and was independent of size. Interestingly, upon closer examination of their self-consistent tight-binding calculation results,[18] the PL energy in the Si crystallites of diameters below 1.0 nm was estimated to approximately 2.6 eV (480 nm).[19] The PL energy and their size were very similar to that of the presented Si molecular clusters (2.64−2.61 eV (470−475 nm) in 30−400 °C), whose estimated diameters were 0.82−0.74 nm. At this point, the authors tentatively propose that the photoluminescence in the present Si QD thin films originated from the Si=O bond at the Si/SiO_2 interface in the oxidized Si QD, where the Si molecular clusters are embedded in the SiO_2 matrix and modeled by the outer surfaces of the Si=O bonds (Figure 6b). At a curing temperature of 800 °C, a PL intensity was not observed, indicating complete disappearance of the silicon molecule cluster and elimination of the Si=O bonds. Still, nobody, including the authors, has explicitly confirmed the existence of the Si molecular cluster of a diameter near 0.8 nm and PL energy near 2.6 eV. Therefore, it is very reasonable to suggest to theoretical scientists a more sophisticated quantum mechanical calculation-based investigation into the electronic states of such small Si molecular clusters possessing Si=O bonds.

In order to confirm the presence of the Si phases (designated Si molecular cluster) surrounded by the SiO_2 phases, TEM micrographs were obtained for the respective Si QD thin films cured at 30, 80, 400, and 800 °C, as shown in Figure 8. While the crystallinity of the Si-wafer substrate is clearly visible in the TEM images, typical amorphous SiO_2 phases are shown in the Si QD thin films without showing any crystallinity attributable to the Si phases. In order for a material to demonstrate a distinct phase in the TEM inspections, the mass−thickness contrast or diffraction contrast should be

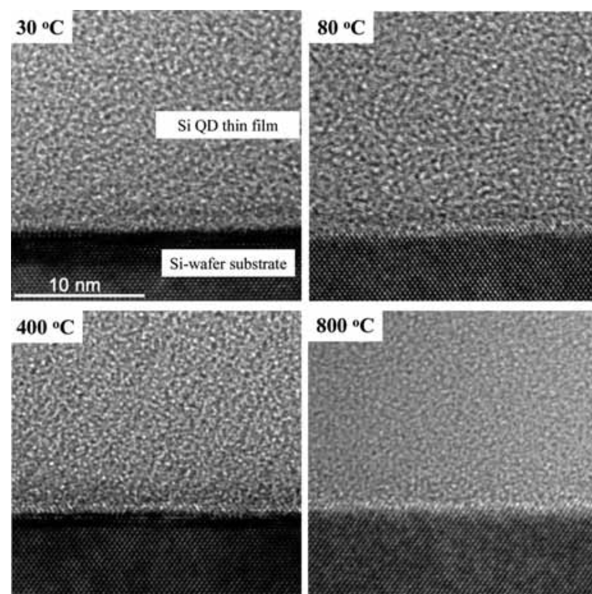

Figure 8. TEM micrographs for the Si QD thin films cured at 30, 80, 400, and 800 °C.

(16) Allan, G.; Niquet, Y. M.; Delerue, C. *Appl. Phys. Lett.* **2000**, *77*, 639.
(17) Koch, F.; Petrova-Koch, V. *J. Non-Cryst. Solids* **1996**, *198*−*200*, 840.
(18) Wolkin, M. V.; Jorne, J.; Fauchet, P. M. *Phys. Rev. Lett.* **1999**, *82*, 197.

(19) See Figure 3 in reference 18.

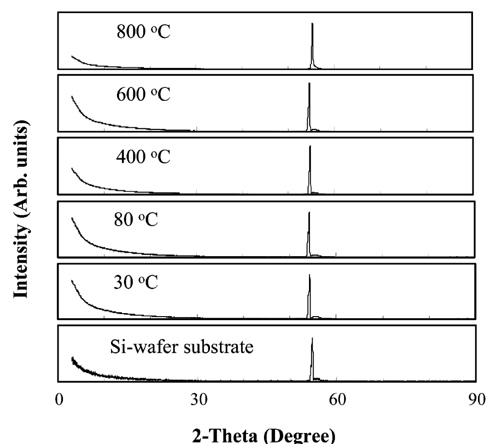

Figure 9. XRD patterns of the Si QD thin films cured at 30, 80, 400, 600, and 800 °C.

sufficiently high.[20] First, within the thin films herein, the Si phases were dispersed randomly in an amorphous SiO_2 matrix, without making any column-like structures throughout the thin films that could enhance contrast for a distinct phase in the TEM images. Additionally, their sizes were very small, with designated "Si molecular clusters" of a diameter of approximately 0.8 nm. As a result, the mass−thickness contrast in the presented thin films was too weak to give a distinct phase in the TEM images. Second, even in the case of weak mass−thickness contrast, alternatively, high diffraction contrast due to the existence of a crystalline structure could give rise to a distinct phase in the TEM images. Nevertheless, as the authors propose consistently throughout our paper, the silicon phases in these films are thought to originate from the Si molecular clusters consisting of roughly 14 silicon atoms, where a domain showing periodicity in the Si atom arrangements is hardly defined, which is prerequisite for the diffraction contrast. Then, there could not be distinct phases due to the diffraction contrast in the TEM images. These arguments are the tentative answers to the question, why the silicon phases are not distinctively discriminated from the ordinary SiO_2 phases in the TEM images. Figure 9 shows XRD patterns for the Si QD thin films cured at 30, 80, 400, 600, and 800 °C, respectively. The results showed only one peak near 56°, assigned to the (311) plane of the Si-wafer substrate without any other significant peaks, confirming that the Si QD thin films had no crystalline phases.

In all likelihood, it is difficult to contend that after severe oxidation, leaving a very small Si phase, all phases are of the same size. Thus, it becomes paramount to discuss the issue of size distribution. There should be statistical variations in the size of the Si phases, although experimental confirmation would be capricious, given its aforementioned subnanometer size in the above TEM results. The diameter value of the Si phases reported in this article is assuredly an average with some variances. Therefore, the silicon molecular cluster consisting of 14 Si atoms can be regarded as a typical, tentative model of the small Si phases, providing a basis for further research. In spite of this, the possibility of the presence of the small Si phases is certain because ordinary silicon oxide materials cannot have such high refractive indices (Figure 4) without involving the Si phases.

The oxidized Si QD films presented herein, which were more evidently pictured as silicon molecular cluster-embedded SiO_2 films, were compared to other silicon superlattice structures within SiO_2[21−24] or SiN,[25−27] which were applied for silicon tandem cells, silicon laser, or light-emitting diodes (LEDs). The advantages of the present Si QD films as silicon superlattice structures were to allow not only low cost but also a large processing area due to solution processability. However, for actual applications, how the size of the Si molecular cluster is controlled has to be first investigated in greater depth from a synthetic and physical chemistry perspective. It is the contention of the authors that the most critical factor for varying the size of the Si molecular cluster is to change the molecular structure of the $SiCl_4$ precursor used in the experiment. In the near future, the structure−properties relationship (molecular structure of the silicon precursors versus size of the embedded Si molecular clusters and resultant optical properties) will be of much interest to material scientists seeking new research opportunities in optoelectronic areas. Another interesting point is that, in semiconductor QDs embedded within dielectrics, the band gap can be tuned, apart from nanocrystal size, by varying the surrounding matrix.[28] This is held to endow a new route to engineer band gaps by varying the chemical composition surrounding the silicon molecular cluster.

Summary

In this study, oxidized Si QD solids in the form of thin films were easily fabricated from the partially oxidized Si QD precursor by a conventional spin-coating method. The oxidized Si QD thin films underwent greater oxidation at increasing curing temperatures, as confirmed by the FT-IR and XPS results. The refractive index value of the Si QD thin film at a 30 °C curing temperature was 1.61, while it was 1.45 for 800 °C, due to complete oxidation of the Si phases. The optical band gap value between 5.49 and 5.90 eV corresponded to the Si phase of a diameter between 0.82 and 0.74 nm, dispersed in the oxidized Si QD thin films, modeled by a Si molecular cluster of close to 14 silicon atoms. The PL energy (2.64−2.61 eV) in the presented Si QD thin films likely originated from the Si═O bond terminating the Si molecular clusters, not the free exciton band gap transition of a nanometer Si QD or Si molecular cluster below 1.0 nm.

Acknowledgment. We thank Mr. Yun Chang Park, a senior member of the measurement and analysis team in the National Nanofab Center, for insightful discussions and assistance with the TEM analysis.

JA9065656

(20) Reimer, L. *Transmission Electron Microscopy*, 4th ed.; Springer: Berlin, 1997; p 197 and p 364.

(21) Photopoulos, P.; Nassiopoulou, A. G.; Kouvatsos, D. N.; Travlos, A. *Mater. Sci. Eng., B* **2000**, *69*, 345.
(22) Frangsuwannarack, T. *Electronic and Optical Characterizations of Silicon Quantum Dots and its Applications in Solar Cells*, Ph.D. Thesis, University of New South Wales, 2007.
(23) Cho, E. C.; Green, M. A.; Conibeer, G.; Song, D.; Cho, Y. H.; Scardera, G.; Huang, S.; Park, S.; Hao, X. J.; Huang, Y.; Dao, L. V. *Adv. Optoelectron.* **2007**, *2007*, 11.
(24) Pavesi, L.; Negro, D.; Mazzoleni, C.; Franzo, G.; Priolo, F. *Nature* **2000**, *408*, 440.
(25) Kim, B. H.; Cho, C. H.; Mun, J. S.; Kwon, M. K.; Park, T. Y.; Kim, J. S.; Byeon, C. C.; Lee, J.; Park, S. J. *Adv. Mater.* **2008**, *20*, 3100.
(26) Park, N. M.; Kim, T. S.; Park, S. J. *Appl. Phys. Lett.* **2001**, *78*, 2575.
(27) Kim, B. H.; Cho, C. H.; Park, S. J.; Park, N. M.; Sung, G. Y. *Appl. Phys. Lett.* **2006**, *89*, 063509.
(28) Nanda, K. K.; Kruis, F.; Fissan, H. *Nano Lett.* **2001**, *11*, 605.